

Posterior predictive model checking using formal methods in a spatio-temporal model

Laura Vana* Ennio Visconti† Laura Nenzi‡ Annalisa Cadonna§
 Gregor Kastner¶

October 5, 2021

Abstract

We propose an interdisciplinary framework, Bayesian formal predictive model checking (Bayes FPMC), which combines Bayesian predictive inference, a well established tool in statistics, with formal verification methods rooting in the computer science community.

Bayesian predictive inference allows for coherently incorporating uncertainty about unknown quantities by making use of methods or models that produce predictive distributions which in turn inform decision problems. By formalizing these problems and the corresponding properties, we can use spatio-temporal reach and escape logic to probabilistically assess their satisfaction. This way, competing models can directly be ranked according to how well they solve the actual problem at hand. The approach is illustrated on an urban mobility application, where the crowdedness in the center of Milan is proxied by aggregated mobile phone traffic data. We specify several desirable spatio-temporal properties related to city crowdedness such as a fault tolerant network or the reachability of hospitals. After verifying these properties on draws from the posterior predictive distributions, we compare several spatio-temporal Bayesian models based on their overall and property-based predictive performance.

Keywords: Bayesian predictive inference, Bayesian spatio-temporal model, formal verification methods, posterior predictive verification, urban mobility

*Corresponding author. Email: ivanague@tuwien.ac.at. Institute of Statistics and Mathematical Methods in Economics, TU Wien, Austria

†ennio.visconti@tuwien.ac.at, Institute of Computer Engineering, TU Wien, Austria

‡laura.nenzi@tuwien.ac.at, Institute of Computer Engineering, TU Wien, Austria

§annalisa.cadonna@gmail.com

¶gregor.kastner@aau.ac.at, Department of Statistics, University of Klagenfurt, Austria

1 Introduction

In this paper, we combine Bayesian inference with formal verification methods widely employed in the computer science literature to specify, verify and evaluate requirements or properties that a spatio-temporal measure of population crowdedness shall satisfy for different decision problems. This interdisciplinary framework provides a unifying approach to the modeling and statistical analysis of data that coherently accounts for uncertainty through the Bayesian paradigm and can be directly employed for decision-making by incorporating application- and decision-specific requirements into the model assessment procedure.

Bayesian predictive inference allows to coherently account for uncertainty about an unknown or future value of a random variable being modeled by providing the entire posterior predictive distribution. Posterior predictive model evaluation and checking (Rubin, 1984) is then employed to check the predictive performance of a Bayesian model on unseen data by qualitatively and quantitatively assessing how well the posterior predictive distributions produced by a model reflect existing data. Formally, from a decision theoretic point of view, the predictive performance of a model is typically defined in terms of a utility or scoring function that measures the quality of the predictive distribution of candidate models (Bernardo and Smith, 1994). Especially when a temporal component is present both in the data and in the modeling framework, the posterior predictive distribution for different time intervals will inform a series of decision problems. Clearly, in the decision-making process, these future values are unknown ex-ante but will be observed ex-post, i.e., after the decision has been taken, so competing models can be compared based on evaluating the out-of-sample posterior predictive distribution given the future observed values. These predictive distributions can be obtained either in an exact fashion, by employing a (time-series) cross-validation where the model is re-estimated as new observations come in, or in an approximate fashion (see e.g., Vehtari et al., 2017; Bürkner et al., 2020). A large body of literature has been concerned with how models should be evaluated and compared based on these predictive distributions, with various versions of predictive density scores being proposed (see, e.g. Corradi and Swanson,

2006; Geweke and Amisano, 2010; Frazier et al., 2021).

Ideally, the score functions or rules employed in the model assessment should be specifically tailored for the application at hand, and the model assessment and comparison should take into account the process through which the prediction of future data with the model enters a decision. However, such approaches are rather limited in the literature, where commonly used measures based on e.g., logarithmic scores are chosen for their desirable mathematical properties. Indeed, in most applications predictions obtained from a (Bayesian) model are often not directly translated into a decision but rather transformed, compressed, and combined with further rules or requirements relevant for the decision problem at hand. As a simple example, consider an algorithmic trading scheme using a predictive model for stock returns which will use the output of the predictive model together with the rule “place a sell order if the 90% quantile of the predictive stock return distribution exceeds 10% three days in a row”. Or a traffic officer who will decide to divert traffic if the model predicts crowdedness to raise above a certain threshold along the city’s main arteries. Such rules could also be employed to put monitoring systems in place for the predictive models (especially black-box ones); e.g., for the purpose of ensuring fairness in the predictions. Especially in high-dimensional, complex models, these requirements or properties relevant for decision-making are typically highly nonlinear functions of the random variables, and one is interested in their predictive distribution. Their verification ex-ante as well as their evaluation ex-post (as part of the posterior model checking and comparison exercise) could provide valuable insights to the modeler and decision-maker and could tailor the analysis to the concrete needs of the decision problem.

We advocate in this paper for the formulation and verification of complex spatio-temporal properties as part of the Bayesian workflow in data analysis. We achieve this by leveraging an existing stream of literature in the computer science field of model checking and verification to approximate the posterior predictive probability of satisfaction of these properties as well as a posterior predictive measure of property reliability or robustness. We then introduce

measures for comparing a collection of spatio-temporal Bayesian models in terms of their ability to predict these quantities, which can complement common predictive evaluation measures such as the log predictive density scores. In the computation of these methods we rely on draws Bayesian predictive distribution, which are obtained through the Markov chain Monte Carlo (MCMC) algorithms employed for parameter estimation.

In order to provide a general framework for the formulation and verification of the requirements we employ formal verification methods, which have a long-standing tradition in the computer science community. Verification methods have historically emerged in the context of hardware and software systems to provide strong guarantees about the correctness of the analyzed implementation concerning a particular high-level formal specification. The traditional approach for formal verification of stochastic systems is probabilistic model checking (introduced independently by [Clarke and Emerson, 1982](#); [Queille and Sifakis, 1982](#)), where the system is described as a finite-state model, on which an exhaustive exploration of the transition space is performed, based on the possible inputs. However, in the context of very large stochastic systems, numerical probabilistic model checking is practically infeasible, and alternative approaches must be taken into account ([Younes et al., 2006](#)). Statistical model checking (SMC, see [Legay et al., 2019](#), for a recent survey on the area) is a simulation based version of probabilistic model checking, where a finite set of trajectories (or system realizations) is used to assess the system's reliability. Complex properties are translated into logical formulae, which can then be automatically verified using efficient algorithms tailored to the type of logic employed. The primary advantage of specifying properties as logic formulae comes from the efficient monitoring algorithms that are available to automatically check whether the specified properties are satisfied or not and to which extent for a given trajectory. Given its scalability and parallelizable nature, SMC has therefore become increasingly used in different application domains especially related to biological systems and cyber-physical systems (see [Nenzi et al., 2017](#), for an application of a continuous time Markov chain model to model a bike sharing system). Extensions to SMC have been proposed, such as Bayesian

SMC (Zuliani et al., 2013) which employs a Beta-Binomial model to incorporate prior information about the probability of satisfaction of a property. However, to the best of our knowledge, existing work in the SMC community does not place emphasis on modeling or uncertainty quantification, as the finite set of trajectories is typically simulated from a model with fixed parameter values. Therefore, a further contribution of our proposed approach is the extension of the classical approach to SMC to a Bayesian framework (which is not to be confused with the aforementioned Bayesian SMC). This is achieved by performing verification and monitoring on a finite set of trajectories from the out-of-sample Bayesian predictive distribution resulting drawn using the MCMC algorithm employed for model estimation.

We illustrate the approach on a spatio-temporal urban mobility application, given that urban population density dynamics are highly variable both in space and time. In this application, building a Bayesian spatio-temporal model able to accurately predict future population dynamics, is of paramount importance to decision-makers in the context of urban planning (e.g., who must plan for resource allocation, divert traffic and increase mobile network capabilities temporarily) but has far-reaching implications related to the environment, economy, and health (Gariazzo et al., 2019). In particular the latter link became even more evident in the context of the COVID-19 pandemic. Analyzing mobile phone traffic data as a proxy for population mobility has been widely employed in the past years (e.g., Deville et al., 2014; Peters-Anders et al., 2017; Gariazzo et al., 2019; Bernini et al., 2019, and references therein) with applications ranging from population density estimation in the absence of census data (Wardrop et al., 2018) to traffic prediction (e.g., Iqbal et al., 2014) and to modeling the spread of epidemics (e.g., Cinnamon et al., 2016; Bonato et al., 2020). Given the high-dimensionality of the mobile phone data, only few studies have focused on sophisticated (Bayesian) modeling tools in an urban planning context. Cadonna et al. (2019) build a spatio-temporal model with spatial clustering of the locations in Milan using data from an Italian telecommunications company; Wang et al. (2021) conducted an empirical study in Shenzhen, China where they include the population statistics and indices for mixed-use to

explore the spatial pattern of population fluctuation in a Bayesian model. For illustration purposes we employ in this work open source data from the “Telecom Italia Big Data Challenge”, which contains telecommunications activity aggregated over a fixed spatial grid of the city of Milan during the months of November and December 2013. Our results provide a deeper understanding of urban dynamics in Milan in terms of the best performing model which identifies areal clusters and in terms of property satisfaction.

The paper is organized as follows: the Bayesian models which will be investigated in the predictive exercise, including a spatio-temporal model with clustering on the areal units, are presented in Section 2. Section 3 presents the Bayesian predictive distribution, provides a description of formal methods and introduces measures for predictive evaluation in terms of property satisfaction. The spatio-temporal properties which are to be verified are introduced in Section 4. The empirical data and results are presented in Section 5. Section 6 concludes and outlines directions of future work.

2 Models

We employ in our analysis several Bayesian models to model the behavior of city crowdedness observed at regular time intervals on a fixed grid area. Let $y_{i,t}$ denote the crowdedness measure in area i at time t for $i = 1, \dots, I$ areas and $t = 1, \dots, T$ time points. The measure is likely to exhibit highly seasonal behavior on both a daily and weekly level. Crowdedness will peak in most areas at noon or in the evening and will drop significantly during the night. Moreover, certain areas will exhibit high activity during the weekdays while others will get crowded during the weekend. We account for such characteristics in the model formulation by employing the following dynamic harmonic regression:

$$\log(y_{i,t}) = \beta_0 + \mathbf{h}_t^\top \boldsymbol{\beta}_i + \eta_{i,t}$$

where β_i is a vector of area-specific regression coefficients, $\eta_{i,t}$ is an error term and $\mathbf{h}_t = (\cos(2\pi\omega_{k_1}t), \sin(2\pi\omega_{k_1}t), \dots, \cos(2\pi\omega_Kt), \sin(2\pi\omega_Kt))^\top$ is a vector of dimension $2K$ of harmonic regressors. The term $\omega_k = k/T$ is a Fourier frequency for which the associated sinusoid completes an integer number of cycles in the observed length of time series and K cannot be larger than $T/2$. Which frequencies shall be included in the covariate matrix can be decided by inspecting the periodograms of the time series for each location i (for a picture of the periodogram for the application at hand see Figure 4 in Section 5).

Baseline model The simplest model considered is a harmonic regression where we assume that the dependence in crowdedness is explained by the harmonic regressors and with error term $\eta_{i,t} \stackrel{iid}{\sim} \mathcal{N}(0, \sigma^2)$. Moreover, we assume that all spatial units share the same temporal behavior with $\beta_i \equiv \beta$.

CAR-AR models with common harmonic regression coefficients The error term $\eta_{i,t}$ is split into two components:

$$\eta_{i,t} = w_{i,t} + \epsilon_{i,t},$$

where $\epsilon_{i,t}$ is normally distributed $\epsilon_{i,t} \stackrel{iid}{\sim} \mathcal{N}(0, \sigma^2)$ and $w_{i,t}$ is a space-time random effect which captures the spatio-temporal dependence in the log crowdedness measure unexplained by the Fourier covariates. The random effect $w_{i,t}$ is modeled as a stationary first-order auto-regressive process:

$$w_{i,t} = \xi w_{i,t-1} + \sqrt{1 - \xi^2} u_{i,t}, \quad t = 2, \dots, T, \quad (1)$$

where $\xi \in (-1, 1)$ to ensure stationarity of the model and $u_{i,t}$ is a mean zero stationary spatial innovation process with variance τ^2 which is independent over time but correlated over the spatial units:

$$\mathbf{u}_t \stackrel{iid}{\sim} \mathcal{N}(\mathbf{0}, \tau^2 Q(\rho, W)^{-1}).$$

For the first time point we have $\mathbf{w}_1 \sim \mathcal{N}(\mathbf{0}, \tau^2 Q(\rho, W)^{-1})$. The matrix $Q(\rho, W)$ denotes the spatial precision proposed in [Leroux et al. \(2000\)](#):

$$Q(\rho, W) = \rho(\text{diag}(W\mathbf{1}) - W) + (1 - \rho)\mathbb{I},$$

where $\mathbf{1}$ is the $I \times 1$ vector of ones while \mathbb{I} is the $I \times I$ identity matrix. In this spatial prior, $0 \leq \rho \leq 1$ provides a measure of spatial dependence while the spatial auto-correlation is controlled by the symmetric $I \times I$ adjacency matrix W , where w_{kl} is equal to one if area k shares an edge or a vertex with area l and zero otherwise (the so-called queen contiguity). This mean-zero normal prior on the spatial innovations is referred to in the literature as a spatial conditionally auto-regressive (CAR) prior. We assume $\boldsymbol{\beta}_i \equiv \boldsymbol{\beta}$.

CAR-AR model with spatial clustering (CAR-AR-BNP) We modify the model introduced above in order to identify areas with similar seasonality pattern. We place a Bayesian non-parametric (BNP) Dirichlet process prior on the $\boldsymbol{\beta}_i$ coefficients for all locations:

$$\boldsymbol{\beta}_i | P \stackrel{iid}{\sim} P, \quad i = 1, \dots, I, \text{ with } P \sim \text{DP}(\alpha, P^0), \quad P(\cdot) = \sum_{j=1}^{\infty} \pi_j \delta_{\boldsymbol{\theta}_j}(\cdot), \quad (2)$$

where the random measure P is represented as the infinite sum of the product of random weights π_j and locations $\boldsymbol{\theta}_j \sim P^0$ and $\delta_{\boldsymbol{\theta}}$ represents the point mass at $\boldsymbol{\theta}$. The stick breaking prior is assumed on the common weights $\pi_j / \prod_{i=1}^{j-1} (1 - \pi_i) \sim \text{Beta}(1, \alpha)$ and the reference measure is specified as $P^0(\boldsymbol{\beta}) = \mathcal{N}_{2K}(\boldsymbol{\beta} | \boldsymbol{\mu}_0, \Sigma_0)$.

Further priors and estimation The intercept term β_0 has a mean zero normal prior. For the models with one set of regression coefficients we employ $\boldsymbol{\beta} \sim \mathcal{N}_{2K}(\boldsymbol{\beta} | \boldsymbol{\mu}_0, \Sigma_0)$. Uniform priors are set on ρ and ξ and inverse Gamma conjugate priors are set for the variance parameters: $\sigma^2 \sim \mathcal{IG}(a^\sigma, b^\sigma)$ and $\tau^2 \sim \mathcal{IG}(a^\tau, b^\tau)$.¹

Inference is performed using MCMC methods. The CAR-AR models are Gaussian state

¹These component specifications, along with our a-priori independence assumption, form the joint prior.

space models where the full conditional distributions of the parameters have a closed form so a Gibbs sampler can be employed. A rough outline of the samplers is given below:

1. For CAR-AR-BNP: The marginalized sampler together with the reuse algorithm in [Favaro and Teh \(2013\)](#) is implemented for sampling the cluster assignments and the unique values of the cluster parameters (see [Cadonna et al., 2019](#)).
2. The unique values of the regression coefficients are sampled from the full conditional.
3. Sample the spatio-temporal random effects $w_{i,t}$ efficiently from an $I \times T$ multivariate normal distribution by exploiting the sparsity of the spatial precision matrix.
4. Parameters ρ and ξ are sampled from a truncated normal distribution on the intervals $[0, 1]$ and $[-1, 1]$, respectively.
5. Variance parameters τ^2 and σ^2 are sampled from the respective conjugate full conditional posterior distribution.

3 Predictive performance assessment and predictive verification

After presenting the Bayesian predictive distribution and the log predictive density scores as ex-post predictive evaluation measures, we introduce formal verification methods in general and spatio-temporal reach and escape logic (STREL, [Bartocci et al., 2017](#)) as the language used for specifying properties in particular. We conclude this section by introducing two Bayesian posterior predictive quantities derived from the formal verification method, namely the posterior predictive satisfaction and robustness. As a framework for predictive inference, we assume the observations up to time $t < T$ are used as a training sample and the evaluation is performed on the observations at the remaining $t + 1, \dots, T$ time points.

3.1 Bayesian predictive distribution and log predictive density scores

The h -step ahead Bayesian predictive density is given by

$$p(\mathbf{y}_{t+h}^o | \mathbf{y}_{1:t}^o) = \int_{\mathcal{K}} p(\mathbf{y}_{t+h}^o | \mathbf{y}_{1:t}^o, \boldsymbol{\kappa}) p(\boldsymbol{\kappa} | \mathbf{y}_{1:t}^o) d\boldsymbol{\kappa}, \quad (3)$$

where $\mathbf{y}_{1:t}^o$ denotes the observed values of $\mathbf{y}_{1:t} = (\mathbf{y}_1, \dots, \mathbf{y}_t)$, each being I dimensional random variables, $\boldsymbol{\kappa}$ contains all parameters and latent quantities to be estimated, $p(\boldsymbol{\kappa} | \mathbf{y}_{1:t}^o)$ denotes their posterior distribution and \mathcal{K} contains the corresponding integration space. It can be seen that the predictive density in Equation (3) is given by the integral of the likelihood function where the values of the unobservables $\boldsymbol{\kappa}$ are weighted according to their posterior distribution. This means that this predictive density integrates uncertainty about the vector of unobservables and the intrinsic uncertainty about the future value \mathbf{y}_{t+h} given the history $\mathbf{y}_{1:t}^o$.

The posterior distribution $p(\boldsymbol{\kappa} | \mathbf{y}_{1:t}^o)$ can be accessed by generating M draws $\boldsymbol{\kappa}_{1:t}^{(m)}$ from the posterior up to time t using the MCMC algorithm outlined in Section 2. The predictive distribution in Equation (3) can then be accessed by simulating $\mathbf{y}_{t+h}^{(m)}$ from each of the distributions represented by the (in our model multivariate Gaussian) density $p(\mathbf{y}_{t+h}^o | \mathbf{y}_{1:t}^o, \boldsymbol{\kappa}_{1:t}^{(m)})$ for $m = 1, \dots, M$.

The Bayesian predictive distribution in Equation (3) can also be employed for the purpose of model comparison and model evaluation by using the h -steps ahead log predictive density scores (cf., e.g., [Geweke and Amisano, 2010](#); [Kastner, 2016](#)). If we evaluate (3) at the observed value \mathbf{y}_{t+h}^o , the h step ahead LPDS is the real number:

$$\text{LPDS}_{t+h} = \log \int_{\mathcal{K}} p(\mathbf{y}_{t+h}^o | \mathbf{y}_{1:t}^o, \boldsymbol{\kappa}) p(\boldsymbol{\kappa} | \mathbf{y}_{1:t}^o) d\boldsymbol{\kappa} \approx \log \left(\frac{1}{M} \sum_{m=1}^M p(\mathbf{y}_{t+h}^o | \mathbf{y}_{1:t}^o, \boldsymbol{\kappa}_{1:t}^{(m)}) \right).$$

3.2 Formal verification methods – STREL

With the goal of incorporating application-specific properties into the Bayesian workflow, we introduce formal verification methods as a way to specify and verify such requirements.

A formal verification method has the goal of checking whether a (stochastic) system satisfies some properties or requirements, which are stated in a formal language. In our case, we consider as a formal language STREL (spatio-temporal reach and escape logic [Bartocci et al., 2017](#)). A spatio-temporal logic combines atomic propositions via a set of operators: the standard Boolean operators ($\vee, \neg, \rightarrow, \dots$), temporal operators to specify the temporal evolution and spatial operators to reason about the space. Let us now describe the language more in detail. Recall from Section 2 that we denote with $i = 1, \dots, I$ the areas (or cells) of the city grid. The logic requires a spatial configuration, which in our application is the one defined through the adjacency matrix W in Section 2 and the distance between two cells i and j is the path that minimizes the number of “hops” or “jumps” from cell i to cell j . On this spatial configuration, we can define various properties which combine different requirements on relevant spatio-temporal quantities. The framework is rather general, but we are primarily interested in the properties in a predictive context so we will formulate and consider requirements on the future crowdedness values up to h -steps ahead $\mathbf{y}_{t+1:h} = (\mathbf{y}_{t+1}, \dots, \mathbf{y}_{t+h})$. The logic formulae are then specified with the language generated by the following grammar, which defines rules for building formulae recursively starting from the atomic proposition:

$$\varphi ::= y \leq c \mid \neg \varphi \mid \varphi_1 \rightarrow \varphi_2 \mid F_{\leq h} \varphi \mid G_{\leq h} \varphi \mid \varphi_1 \mathcal{R}_{\leq d} \varphi_2 \mid \diamondsuit_{\leq d} \varphi. \quad (4)$$

The atomic propositions in STREL are defined as inequalities between the quantity y (i.e., crowdedness) and the real-valued constant c , e.g. $y < c$ or $y > c$. Boolean operators like \neg and \rightarrow denote the classical logical operations of negation and implication. We use $F_{\leq h} \varphi$ and $G_{\leq h} \varphi$ as fundamental temporal operators, the former denoting the occurrence of property φ

in at least once in the future time interval $(t, t + h]$ (i.e., the eventually operator), and the latter corresponding to the occurrence of property φ in all future time points in the interval $(t, t + h]$ (i.e., the globally operator).² When the context requires also lower-bounds to the times of interest, we will adopt an interval-based notation, like $F_{[a,b]}$ or $G_{[a,b]}$ to denote the interval $[t + a, t + b]$.³ Lastly, spatial operators are represented by $\varphi_1 \mathcal{R}_{\leq d} \varphi_2$ and $\diamondsuit_{\leq d} \varphi$. The former denotes the reachability of an area where φ_2 holds from an area where φ_1 holds, at a distance smaller or equal than d . The latter corresponds to the notion of somewhere, denoting the presence of at least one area at a distance smaller or equal than d where φ holds.

Once the properties are specified as logic formulae, efficient algorithms are available to approximate the behavior of the stochastic system with respect to the properties. One is interested firstly in the satisfaction $S(\mathbf{y}_{t+1:h}, \varphi)$, i.e., whether the quantities of interest, e.g., $\mathbf{y}_{t+1:h}$, satisfy property φ (here φ also contains property parameters such as c, h, d in Equation (4)). Secondly, the robustness function $R(\mathbf{y}_{t+1:h}, \varphi)$ (Fainekos and Pappas, 2009) is defined as the bound on the perturbation that the quantities of interest can tolerate without changing the truth value of a property, which can be interpreted as a measure of reliability. The advantage of specifying properties in terms of logical operators lies in the existence of efficient monitoring algorithms tailored to the type of logic employed. Given realizations of the system, these automatically check whether the system satisfies the properties, and to which extent. More specifically, STREL comes with two monitoring algorithms. First, the Boolean one. It returns a yes/no answer while checking for the satisfaction of a given formula on a specific trajectory. Second, the quantitative one, which computes the value of the robustness function for a given realization. The robustness function is defined for each

²Given the discrete time points of the quantities of interest, we assume a constant behavior in between time points $t+1, \dots, t+h$. On a technical note, following standard practice in the formal verification literature, we assume in the same fashion that from time t up to time $t+1$ the process stays constant. This implies that for checking the validity of the temporal properties over the whole interval $(t, t + h]$, the variable \mathbf{y}_t is also considered a relevant quantity. We however omit this quantity from the exposition, to not detract the reader from the focus on the predictive aspect of the framework.

³Note that for sake of keeping notation simple we omit t from the definition of the temporal operators.

logical operator,⁴ with a positive value corresponding to satisfaction and a negative value to violation of the property.

We refer the interested reader to [Bartocci et al. \(2017\)](#) for a complete and formal description of the logic, or to [Nenzi et al. \(2020\)](#) for a more comprehensive list of case studies, while we devote the rest of this section to highlighting the key benefits of adopting the STREL machinery for property verification. The primary advantage is that STREL is a specification language crafted specifically for keeping a strong connection with intuitive notions of spatial and temporal concepts, allowing to express extremely complex requirements in a compact and understandable way.⁵ Moreover, a key advantage of specifying requirements in terms of STREL operators is that the Moonlight⁶ software is readily available for automatically verifying that a given set of signals satisfies (or violates) the provided specification. Lastly, it must be noted that the automatic monitoring of STREL specification implemented by Moonlight takes into account state-of-the-art algorithms for maximizing memory and computational time efficiency (with usually better performances than alternatives). While ad-hoc algorithms can be more efficient if they are tailored to a given specification, they are often costly to adapt as the requirements and monitored properties evolve. Therefore, the generality offered by the framework and the Moonlight software ensure easy adaptability of the property specifications with minimal changes from the part of the modeler.

3.3 Predictive model checking using formal methods

In the following we show how the formal verification methods introduced above can be utilized in a natural way in a context where the stochastic system is defined following the Bayesian paradigm and how such methods complement posterior predictive inference and

⁴In the simple case of the atomic proposition, the robustness is given by the difference between the quantity of interest and the threshold c . For a detailed explanation into the computation of the robustness for the logic operators used in this paper see [Bartocci et al. \(2017\)](#).

⁵Note that a dedicated scripting language for STREL is available. It allows to express the formulae in almost-plain English.

⁶For latest Moonlight development updates and tool instructions, see <https://github.com/moonlightsuite/moonlight>.

model checking. The framework can help statisticians and decision-makers to automatically check whether the system will satisfy or not these properties at a future time point a posteriori. To extend the concept of satisfaction and robustness over the whole stochastic system, we introduce two key concepts i) the Bayesian predictive probability of satisfaction and ii) the expected value of the Bayesian predictive robustness.

The Bayesian h -step-ahead predictive probability of satisfaction for property φ at location i and time t is given by

$$\begin{aligned} \mathbb{E}[S_i(\mathbf{y}_{t+1:h}, \varphi) | \mathbf{y}_{1:t}^o] = \\ \int_{\mathbf{y}_{t+1} \in \mathcal{Y}_1} \dots \int_{\mathbf{y}_{t+h} \in \mathcal{Y}_h} S_i(\mathbf{y}_{t+1:h}, \varphi) p(\mathbf{y}_{t+1:h} | \mathbf{y}_{1:t}^o) d\mathbf{y}_{t+1} \dots d\mathbf{y}_{t+h}. \end{aligned} \quad (5)$$

We can approximate the probability in (5) by using the draws from the Bayesian predictive density,

$$\mathbb{E}[S_i(\mathbf{y}_{t+1:h}, \varphi) | \mathbf{y}_{1:t}^o] \approx \frac{1}{M} S_i(\mathbf{y}_{t+1:h}^{(m)}, \varphi), \quad (6)$$

where for one draw m the $S_i(\mathbf{y}_{t+1:h}^{(m)}, \varphi)$ takes either value zero or value one.

Conditional on the observed data, the Bayesian predictive robustness is a function of the relevant signals for the property φ together with the property parameters. Analogously to above, we investigate in this paper its expected value at location i and time t , which is given by

$$\begin{aligned} \mathbb{E}[R_i(\mathbf{y}_{t+1:h}, \varphi) | \mathbf{y}_{1:t}^o] = \\ \int_{\mathbf{y}_{t+1} \in \mathcal{Y}_1} \dots \int_{\mathbf{y}_{t+h} \in \mathcal{Y}_h} R_i(\mathbf{y}_{t+1:h}, \varphi) p(\mathbf{y}_{t+1}, \dots, \mathbf{y}_{t+h} | \mathbf{y}_{1:t}^o) d\mathbf{y}_{t+1} \dots d\mathbf{y}_{t+h}, \end{aligned} \quad (7)$$

and can be approximated by

$$\mathbb{E}[R_i(\mathbf{y}_{t+1:h}, \varphi) | \mathbf{y}_{1:t}^o] \approx \frac{1}{M} R_i(\mathbf{y}_{t+1:h}^{(m)}, \varphi). \quad (8)$$

The monitoring algorithms of STREL are employed here to efficiently calculate (6) and (8) for the $m = 1, \dots, M$ posterior predictive draws.

These measures can then be employed for the purpose of model comparison and posterior predictive assessment by comparing the posterior predictive satisfaction and robustness measures estimated on the M trajectories with the ex-post evaluation of the satisfaction and robustness of the properties on the observed data $\mathbf{y}_{t+1:h}^o$. We compute for this purpose the following measures:

- Mean accuracy between the observed and estimated satisfaction,

$$\bar{\text{Acc}}_t^{\text{Satisf}} = \frac{1}{M} \sum_{m=1}^M \left(\frac{1}{I} \sum_{i=1}^I 1\{S_i(\mathbf{y}_{t+1:h}^{(m)}, \varphi) = 1\} 1\{S_i(\mathbf{y}_{t+1:h}^o, \varphi) = 1\} \right).$$

- Mean F1 score between the observed and estimated satisfaction,

$$\bar{\text{F1}}_t^{\text{Satisf}} = \frac{1}{M} \sum_{m=1}^M 2 \frac{\text{recall}^{(m)} \times \text{precision}^{(m)}}{\text{recall}^{(m)} + \text{precision}^{(m)}},$$

where

$$\begin{aligned} \text{precision}^{(m)} &= \frac{\sum_{i=1}^I 1\{S_i(\mathbf{y}_{t+1:h}^{(m)}, \varphi) = 1\} 1\{S_i(\mathbf{y}_{t+1:h}^o, \varphi) = 1\}}{\sum_{i=1}^I 1\{S_i(\mathbf{y}_{t+1:h}^{(m)}, \varphi) = 1\}}, \\ \text{recall}^{(m)} &= \frac{\sum_{i=1}^I 1\{S_i(\mathbf{y}_{t+1:h}^{(m)}, \varphi) = 1\} 1\{S_i(\mathbf{y}_{t+1:h}^o, \varphi) = 1\}}{\sum_{i=1}^I 1\{S_i(\mathbf{y}_{t+1:h}^o, \varphi) = 1\}}. \end{aligned}$$

- Root mean squared error (RMSE) between the observed and the estimated robustness,

$$\text{RMSE}_t^{\text{Rob}} = \sqrt{\frac{1}{M} \sum_{m=1}^M \left\{ \frac{1}{I} \sum_{i=1}^I (R_i(\mathbf{y}_{t+1:h}^{(m)}, \varphi) - R_i(\mathbf{y}_{t+1:h}^o, \varphi))^2 \right\}}.$$

4 Crowdedness requirements

4.1 Informal specification of requirements

In this section we propose some informal properties that the crowdedness level in the city grid should satisfy in order to robustly withstand critical events. Let c represent a crowdedness threshold for all the areas of the city.⁷ This threshold would typically be known to the decision-maker and would correspond to the maximum value for which a certain location would still be considered uncrowded. Moreover, let h_φ be a time step in the future to be used in a property or requirement φ . As in the previous section, we assume that we train our Bayesian model using data up to time $t < T$.

Given that the measure of crowdedness we are employing is derived from mobile phone data, one possible stakeholder of our proposed framework is a telecommunications company, which would like to have a predictive alert system to ensure that their mobile network does not get overcrowded. The following three properties could be of interest to the telecommunications company:

P.1 Overloads are temporary: if the level of crowdedness goes above the threshold c in the period following t , then it must return below c latest by time $t + h_{P.1}$.

P.2 Overloads are local: if at a certain location the level of crowdedness at $t + h_{P.2}$ rises above c , this location must be at most at distance $d_{P.2}$ from another location with a level of crowdedness below c at the same time. This is a minimal spatial requirement for a city grid trying to balance excessive loads.

P.3 The network is fault-tolerant: for a location, the level of crowdedness in that location or in other locations within a distance of $d_{P.3}$ should be below c at all times in the interval $(t, t + h_{P.3}]$, i.e., emergency load-balancing must be possible.

⁷Note, however, that the framework can accommodate for e.g., area-specific threshold values. We restrict ourselves to a universal c for the sake of simplicity in the exposition.

In addition to the previous requirements that are related to general aspects of the mobile network, for the evaluation of the city in terms of safety and quality of life, it is interesting to look at how the city is performing with respect to the reachability of some key points of interest. For example, in an emergency scenario, a traffic monitoring body would be interested in the following requirement (assuming that our crowdedness measure is indeed a proxy for population density in the city):

P.4 Uncrowded reachability: A hospital must be reachable within a distance of $d_{P.4}$ from any uncrowded location of the city center, in the time interval $(t, t + h_{P.4}]$, by only going through uncrowded locations.

All of the requirements will be checked for each location in the grid $i = 1, \dots, I$.

4.2 Formalizing the requirements

We show here how to use the STREL presented in Section 3.2 to specify the requirements introduced above. The previous requirements will be in the following formally expressed as STREL formulae, and the key operators will be described gradually. Before looking at the formalization of the requirements, we introduce the atomic property

$$\phi = (y > c)$$

i.e. the crowdedness is above a certain threshold c . Conversely, the formula $\neg\phi$ represents the case where the crowdedness level is below the threshold c . This formula constitutes the basic building block for formalizing our requirements; in fact, the first requirement was related to temporary overloads, which can be formulated by using temporal operators in the following way:

$$\varphi_{P.1} = \phi \rightarrow F_{\leq h_{P.1}} \neg\phi. \quad (P.1)$$

The second property, related to overloads being local, can be formalized as a spatio-temporal property:

$$\varphi_{P.2} = F_{=h_{P.2}}(\phi \rightarrow \Diamond_{\leq d_{P.2}} \neg\phi) \quad (P.2)$$

Note that the temporal operator $F_{=h_{P.2}}$ here denotes that the requirement shall hold at the time which lies $h_{P.2}$ -steps ahead in the future.

Thirdly, the fault-tolerance of the network is a spatio-temporal requirement which can be formulated as:

$$\varphi_{P.3} = G_{\leq h_{P.3}}(\Diamond_{\leq d_{P.3}} \neg\phi) \quad (P.3)$$

where $G_{\leq h_{P.3}}$ requires the “somewhere” property to hold globally for the whole interval $(t, t + h_{P.3}]$.

Lastly, for the requirement related to the reachability of hospitals, let us first introduce a new atomic proposition:

$$\phi_2 = isHospital$$

ϕ_2 is a peculiar proposition representing hospital locations, meaning that it is satisfied only when the current location comprises a hospital. A first, direct translation of the P.4 could be the following:

$$F_{\leq h_{P.4}}(\neg\phi \mathcal{R}_{\leq d_{P.4}} \phi_2)$$

While the previous requirement formalizes P.4 literally, it likely gives an unrealistic interpretation to the requirement. In fact, $\neg\phi \mathcal{R}_{\leq d_{P.4}} \phi_2$ means that a hospital can be reached by only traversing uncrowded areas, however it does not consider the traveling time to reach

the location, meaning that the property would be satisfied whenever there is an uncrowded path to the hospital (although the actual traveling time might be significantly higher). A more realistic (although a bit more involved) version is presented below:

$$\varphi_{P.4} = \varphi_{\alpha,0,d_{P.4}} \quad (P.4)$$

$$\varphi_{\alpha,i,n} = \begin{cases} \phi_2 & n = 0 \\ \phi_2 \vee ((G_{[i,i+1]} \neg \phi) \wedge (\Diamond_{\leq 1} \varphi_{\alpha,i+1,n-1})) & \text{otherwise.} \end{cases}$$

Property $\varphi_{P.4}$, with a slight abuse of notation, encodes our requirement and shows the flexibility of the logic approach. The requirement states that one needs to move at most $d_{P.4}$ cells in the time interval $(t, t + h_{P.4}]$ time units, but it does not explicitly specify how fast one can move through the different cells of the city grid. To give a realistic interpretation to the specification, we assumed that in 10 min one can only travel from one cell to the next. This interpretation translates into $\varphi_{\alpha,n,j}$, which imposes that the current location is not crowded for the next ten minutes, and iteratively enforces this n times by the recursive check of $\varphi_{\beta,n,j}$, until the maximum distance is reached (in terms of “hops” on the grid), in which case it looks for a hospital in the neighborhood. This way analyzing the satisfaction or robustness of $\varphi_{P.4}$, will not only provide insights about the spatial reachability of a hospital, but it will also take into account the traversal time needed to reach it.

5 Empirical illustration

5.1 Data

The almost universal use of mobile phones has generated vast amounts of data mainly in the form of mobile phone location data through the so called call detail records (CDRs),

which are a valuable proxy for population distribution and people's mobility habits (Peters-Anders et al., 2017). The mobile communication service providers generate a CDR whenever a device state changes either because of the user's actions (phoning, texting, browsing on the internet) or because of technical reasons (e.g., switching to cell with stronger signal in the cellular network). The CDR will then record the time and the cell that handled the interaction, data which in turn can be used to obtain an approximate location of the user. This type of information has a high potential in researching the patterns in mobility at a high frequency in time and over a large spatial network.

“Telecom Italia Big Data Challenge” dataset In general, the acquisition of mobile phone data from the telecommunications providers is a rather difficult process primarily due to security and privacy concerns and very few open datasets are available for research. One exception is provided by Telecom Italia's open source data base within the scope of the “Telecom Italia Big Data Challenge”, which contains various geo-referenced, aggregated and anonymized datasets for city of Milan and the Province of Trentino, with the “main” data set containing telecommunications activity data derived from CDRs (for a detailed description see Barlacchi et al., 2015). The datasets are released under the Open Database License (ODbL) and are publicly available in the Harvard Dataverse. The telecommunications activity data covers the period November 01, 2013 to December 16, 2013 and the CDR data provided is aggregated in both space and time. In the case of Milan, the city area is composed of a grid overlay of 1,000 squares with size of approximately 235m×235m with the CDRs being aggregated inside each square. Additionally, a temporal aggregation is performed in time slots of ten minutes. Information on the type of activity which generated the CDR is also provided in the database:

- SMS-in activity: activity proportional to the amount of received short message services (SMSs) inside a given grid square during a given time interval. A CDR is generated each time a user receives an SMS.

- SMS-out activity: activity proportional to the amount of sent SMSs inside a given grid square during a given time interval. A CDR is generated each time a user sends an SMS.
- Call-in activity: activity proportional to the amount of received calls inside a given grid square during a given time interval. A CDR is generated each time a user receives a call.
- Call-out activity: activity proportional to the amount of issued calls inside a given grid square during a given time interval. A CDR is generated each time a user issues a call.
- Internet traffic activity: number of CDRs generated inside a given grid square during a given time interval. A CDR is generated each time a user starts an Internet connection or ends an Internet connection. During the same connection a CDR is generated if the connection lasts for more than 15 min or the user transferred more than 5 MB.

The data is further anonymized by dividing the true number of records in each category by a constant known to Telecom Italia, which hides the true number of calls, SMS and internet connections.

Data description In this application, we illustrate the proposed framework on a subset of the Milan telecommunications activity dataset covering the period November 04, 2013 (Monday) to November 11, 2013 (Monday). We further restrict our analysis to the central 21×21 grid, where the center-most cell is the one containing the location of the Milan Duomo. This grid corresponds to an area of around 25km^2 . Moreover, we consider the sum of all the mobile phone activity measures (i.e., SMS-in, SMS-out, call-in, call-out and internet) as our measure of crowdedness. We use this aggregated measure, because i) the phoning (call-in, call-out) and texting by SMS measures are rather sparse during the night, as people rarely call or text after midnight, ii) the modern use of cell phones relies much more on browsing the internet or on messaging apps which gained popularity around 2010. As such,

considering the internet CDRs in addition to the other four can paint a more realistic picture of the crowdedness of a certain area.

Figure 1 contains the crowdedness measure averaged over the 10 minute time intervals for the whole analyzed period over the 21×21 grid. Areas with high levels of crowdedness are apparent in the central grid squares in the area surrounding the Milan Duomo ③ and in the upper center, where the two main stations are, namely ① Garibaldi Station and ② Central Station. On the other hand, lower activity grid squares such as the ones overlaid on a highly trafficked avenue on the right hand side and right bottom corner of the map can be identified. In order to illustrate the temporal behavior of the crowdedness measure,



Figure 1: Average crowdedness measure over the period November 04, 2013 to November 11, 2013. The x -axis contains the longitude and the y -axis contains the latitude degrees. The marked areas represent: ① Garibaldi Station, ② Central Station, ③ Duomo, ④ Bocconi, ⑤ Navigli.

we present in Figure 2 the time-series of the grid units containing the three representative districts of ③ Duomo, ⑤ Navigli and ④ Bocconi. We observe a larger high activity in

the area of (3) Duomo compared to the other two districts, which peaks around mid-day during the working days and in the early afternoon on the weekends. (5) Navigli on the other hand, which is a district famous for its different types of cafes, restaurants, bars and design shops, exhibits a more uniform behavior among the working and the weekend days, with activity peaking in the evening hours. The grid square containing the (4) Bocconi university exhibits a clear pattern during the working hours and reduced activity levels on the weekends, especially on Sundays. The seasonality in the data can be identified also in

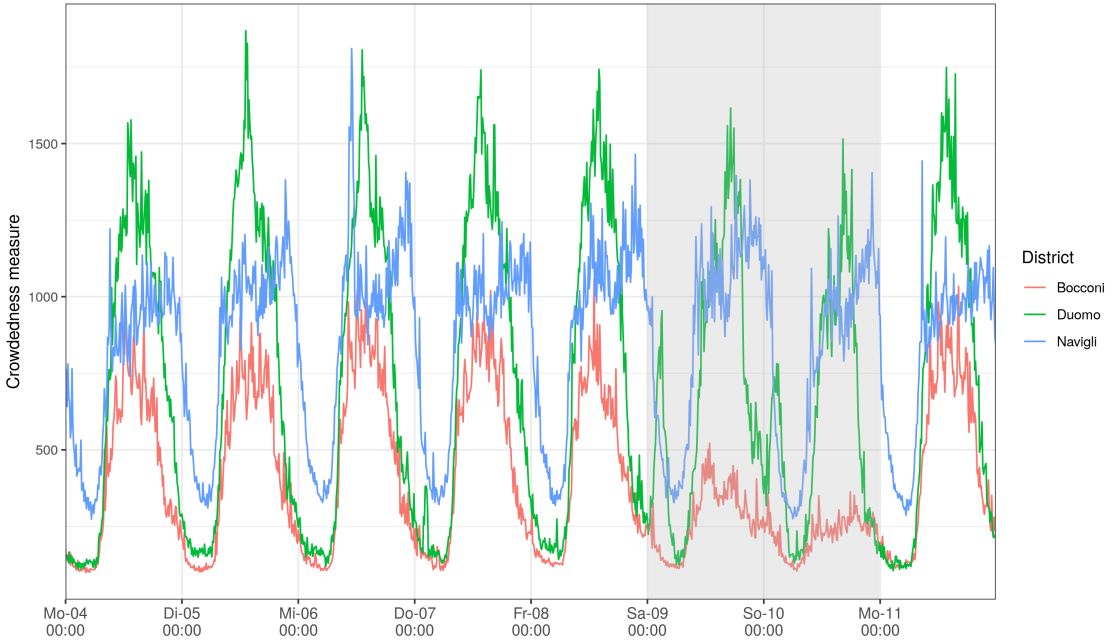


Figure 2: Time series of the crowdedness measure for the areal units containing the districts Duomo, Navigli and Bocconi over the period from November 04, 2013 to November 11, 2013. Areas marked in gray represent weekends.

Figure 3, which contains a visualization of the whole data-set through a raster plot. Aside from the strong daily seasonality which is present in all locations, one can observe different temporal patterns among the areas. Most areas share the characteristic of a relatively lower activity in the weekends, while the activity in the working days differs among groups of locations e.g., the locations from the central part of the grid (cell ids 150–280) exhibit a higher difference between the daily crowdedness during working days vs. weekends, while

locations with cell ids around 400 (top cells in the map) exhibit rather similar activity during the workdays and weekends. Finally, we provide a plot of the estimated spectral densities of

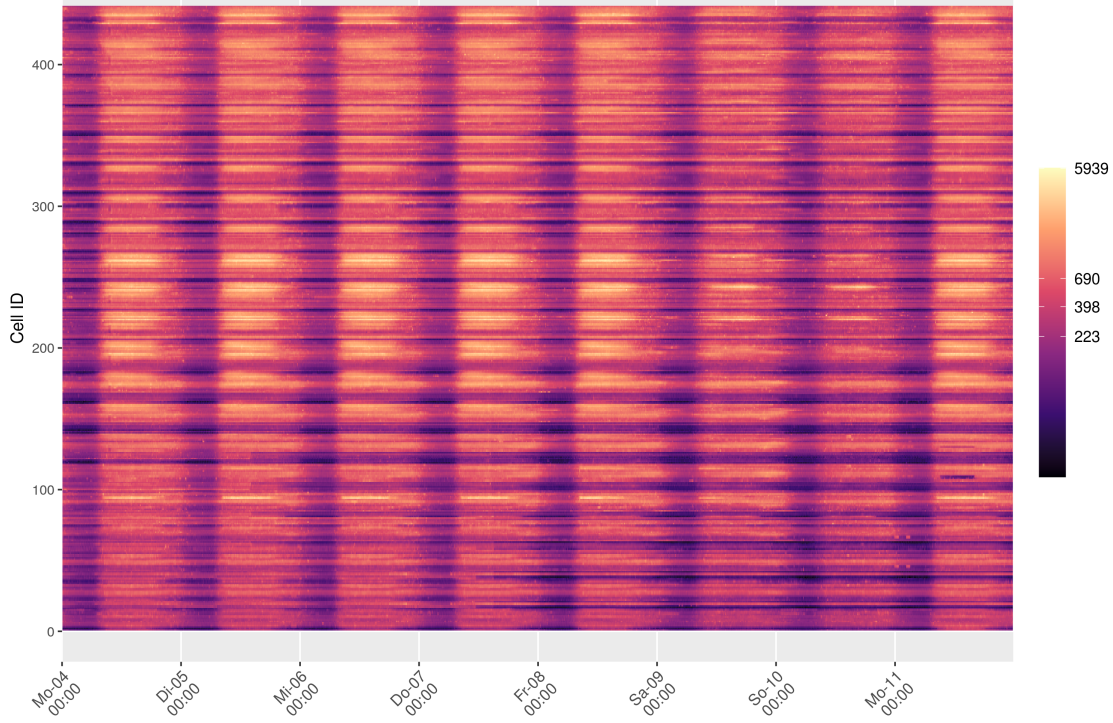


Figure 3: Raster plot exhibiting the time-series of the crowdedness measure for each of the 441 grid squares for the period November 04, 2013 to November 11, 2013.

our $I = 21 \times 21 = 441$ time series in Figure 4. By inspecting these estimates we observe the strong intra-daily as well as a intra-weekly seasonality (given by the large spectral densities at frequencies marked in the graph), with the largest values corresponding to 24 hour intervals. We use this information to select the appropriate frequencies to include in the harmonic regression.

5.2 Model comparison

In the following we investigate and compare the predictive performance of the models introduced in Section 2. For this purpose we set up an out-of-sample exercise based on rolling windows, where we start by training the Bayesian model on data between November 04, 2013 at 00:00 (Monday) and November 10, 2013 23:50 to generate one-, two- and three-step-ahead

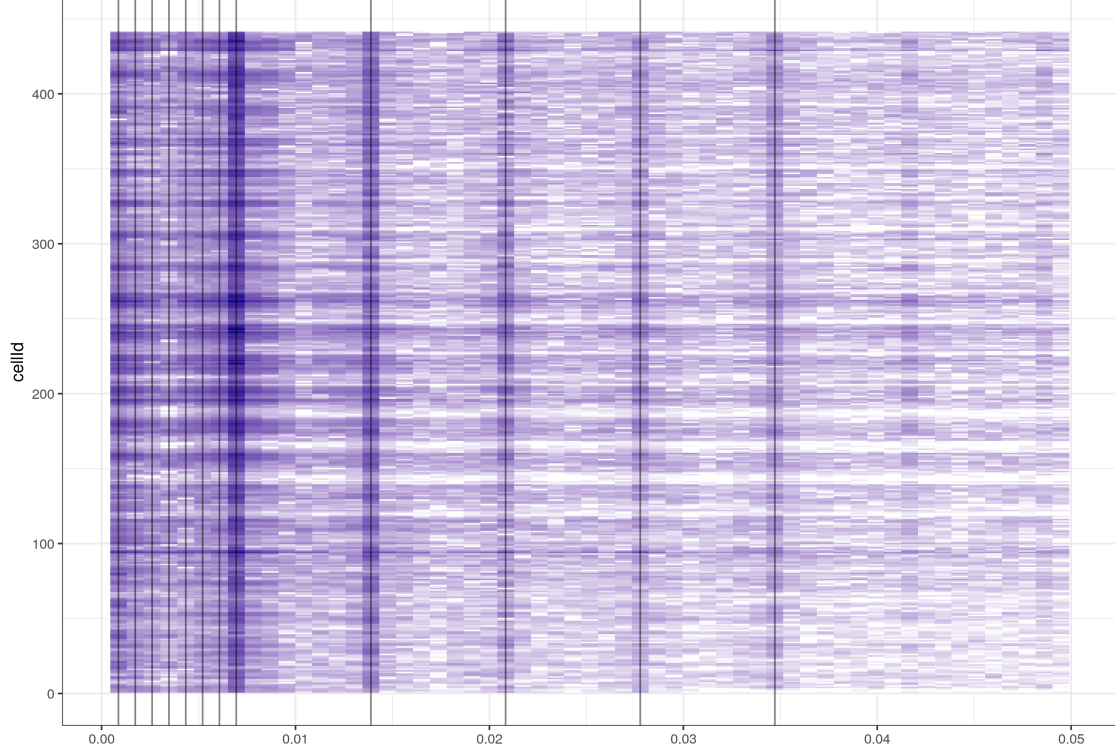


Figure 4: Raster plot exhibiting the spectral density estimates for each of the 441 grid squares for the period from November 04, 2013 to November 11, 2013. The x -axis only exhibits frequencies up to 0.05. The black vertical lines represent the frequencies which were chosen to be included in the harmonic regression after visual inspection of this graph. The chosen frequencies correspond to the intra-weekly and intra-daily seasonality.

predictions, as well as for computing the predictive measures to be used for model selection for November 11, 2013 00:00 up to November 11, 2013 00:20. In a separate estimation procedure we shift the window of the training data by 10 minutes and re-estimate the model in an iterative fashion until we reach the end of the sample.

As mentioned before, as a baseline model we consider the model with no random effects $w_{i,t} = 0$ and with one set of regression coefficients for all locations as the baseline. In addition to the CAR-AR-BNP model which performs clustering on the areal units, we consider three CAR-AR models which all assume a normal prior on β : i) a model where spatial auto-correlation parameter ρ is fixed to 0 (CAR-AR ($\rho = 0$)), ii) a model where spatial auto-correlation parameter ρ is fixed to 0.5 (CAR-AR ($\rho = 0.5$)), iii) a model where the spatial auto-correlation parameter ρ is estimated in the MCMC procedure (CAR-AR).

For all models, the values of the hyper-parameters are kept identical: $\mu_0 = \mathbf{0}$, $\Sigma_0 = 0.1\mathbb{I}_{2K}$, $a^\sigma = a^\tau = 1$, $b^\sigma = b^\tau = 0.01$. We take $\alpha = 1$ in the BNP prior and we use 50 auxiliary variables in the algorithm for sampling the cluster assignments. All results are based on 10000 iterations of the Gibbs sampler, where the first 5000 are discarded as burn-in and the thinning parameter is set to 50.

Figure 5 presents the cumulative one-step-ahead ($h = 1$) and three-step-ahead ($h = 3$) log predictive Bayes factors for Monday, November 11, 2013:

$$\log \text{BF}_{t_1, t_2}(A, B) = \sum_{t=t_1}^{t_2-h} \log \text{LPDS}_{t+h}(A) - \log \text{LPDS}_{t+h}(B)$$

where B is taken to be a baseline model. We observe that all models which take space and/or time correlation into account through the auto-regressive structure outperform the baseline model, with the model CAR-AR-BNP with spatial-clustering also outperforming, even if not by a lot, the CAR-AR model. In terms of the three-steps ahead prediction, the CAR-AR-BNP model is superior, but we observe also that the performance of all CAR-AR models is worse than the baseline in the hours following mid-night and between 07:00-09:00 (see negative slopes in the log Bayes factor curves). Furthermore, the gain in performance of the CAR-AR models diminishes around 19:00, when the slopes of the curves are not as steep. These results point towards the fact that there might be a change in the spatial dependence parameter ρ throughout the day. We leave such an extension of the model to further research.

Finally, we also investigate the performance of the five models in terms of the predictive measures based on property satisfaction and robustness introduced in Section 3.3. The property parameters used for all properties are: $c = 500$, $h_{P.1} = h_{P.3} = 30$ min, $h_{P.2} = 10$ min, $h_{P.4} = 40$ min, $d_{P.2} = d_{P.3} = 1$ cell, $d_{P.4} = 4$ cells. Table 1 shows the posterior mean and standard deviation of the satisfaction accuracy, satisfaction F1 score and robustness RMSE for all four properties. We observe that the CAR-AR-BNP model is the best performing one

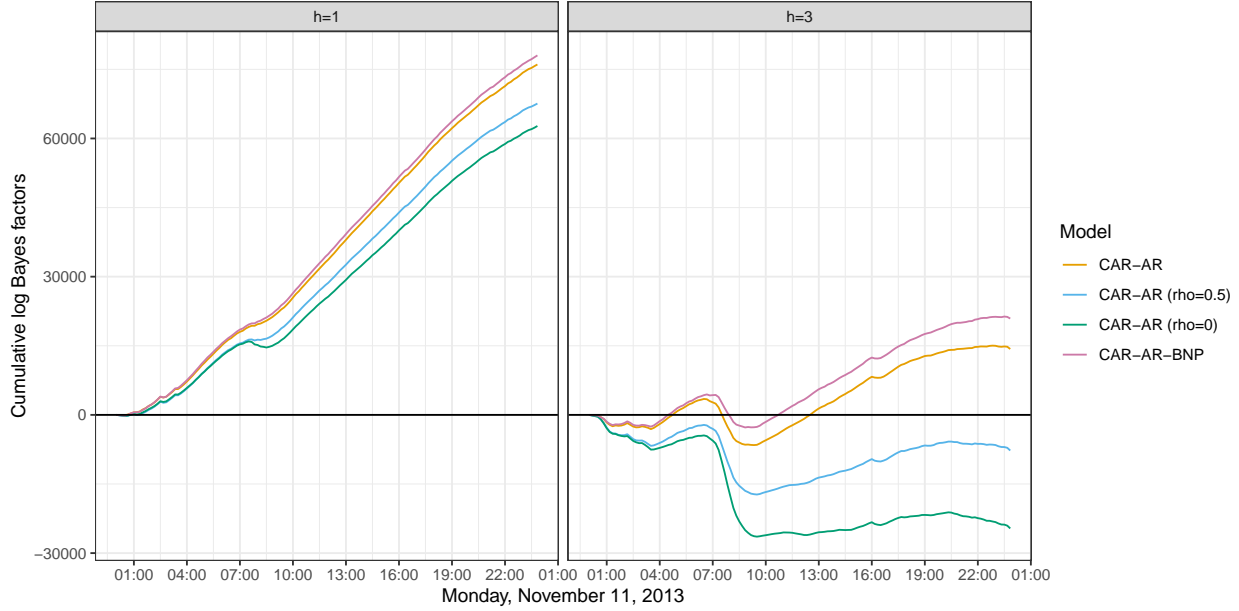


Figure 5: This figure presents one- and three-steps-ahead cumulative log predictive Bayes factors for different models relative to the baseline model.

in terms of the measures inspected, however the difference in performance for some properties is not large. Figure 6 presents the average value of the measures in Table 1 for all testing periods, together with 80% credible intervals. This figure can be used for deciding which model performs best in terms of specific interest in the verified properties. For example, it can be seen that the auto-regressive models perform similarly in terms of satisfaction measures for all properties, while the robustness of the model CAR-AR-BNP is better for properties P.2 and P.3. The same model also outperforms the others in terms of property P.4 during the rush hours 07:00-09:00 so it should be chosen if the performance in this specific time-frame is of interest to the modeler.

5.3 Results of the spatio-temporal model with spatial clustering

The top panel in Figure 7 presents the three clusters identified by employing Binder's loss on the samples of the cluster assignments vector while the bottom panel presents crowdedness measure averaged over all locations in one cluster. The blue cluster is one where the difference in the crowdedness between weekends and working days is not as large as for the other two,

Table 1: This table presents the posterior mean and standard deviation (in parentheses) of the predictive measures of accuracy and F1 scores for property satisfaction and the RMSE of the robustness for the four properties. The reported measures are averages over all test samples.

Measure	Baseline	CAR-AR	CAR-AR	CAR-AR	CAR-AR
		$\rho = 0$	$\rho = 0.5$	BNP	BNP
Property P.1					
\bar{Acc}^{Satisf}	0.6999 (0.0056)	0.944 (0.0025)	0.9479 (0.003)	0.9445 (0.0059)	0.9498 (0.0035)
$\bar{F1}^{Satisf}$	0.8027 (0.0029)	0.9555 (0.0019)	0.9584 (0.0022)	0.956 (0.0043)	0.9601 (0.0026)
$RMSE^{Rob}$	493.2178 (5.84)	101.979 (3.8052)	96.0108 (4.2172)	101.7701 (9.328)	92.9006 (6.104)
Property P.2					
\bar{Acc}^{Satisf}	0.8177 (0.0056)	0.9463 (0.0038)	0.9481 (0.0038)	0.9476 (0.0043)	0.9553 (0.0037)
$\bar{F1}^{Satisf}$	0.8988 (0.0033)	0.9678 (0.0022)	0.9688 (0.0023)	0.9686 (0.0025)	0.9731 (0.0022)
$RMSE^{Rob}$	273.7798 (8.4465)	59.9263 (2.771)	57.5646 (2.5964)	59.1099 (2.7259)	48.6895 (2.8436)
Property P.3					
\bar{Acc}^{Satisf}	0.9116 (0.0076)	0.9511 (0.0028)	0.9508 (0.0031)	0.9515 (0.0036)	0.9547 (0.0039)
$\bar{F1}^{Satisf}$	0.9439 (0.0051)	0.9692 (0.0018)	0.969 (0.0021)	0.9695 (0.0024)	0.9713 (0.0026)
$RMSE^{Rob}$	120.5187 (7.339)	59.3011 (1.9052)	59.1511 (2.8903)	58.645 (3.8598)	52.6133 (3.461)
Property P.4					
\bar{Acc}^{Satisf}	0.9268 (0.0061)	0.9703 (0.0034)	0.9722 (0.0037)	0.9726 (0.0043)	0.9743 (0.0034)
$\bar{F1}^{Satisf}$	0.8575 (0.0117)	0.939 (0.007)	0.9426 (0.0075)	0.9437 (0.0084)	0.947 (0.0068)
$RMSE^{Rob}$	280.6554 (20.4942)	130.225 (6.0651)	125.8994 (5.6114)	128.1106 (6.5048)	122.4351 (5.1467)

with activity peaking the morning (stronger during the working days) as well as in the evening (stronger effect on Sunday). The (5) Navigli area is a member of the blue cluster.

The yellow cluster contains areas where the activity is high in the working days and lower on the weekends, with an intraday peak around noon. Typical locations in this cluster are university centers or the city center where most office buildings are situated. The green cluster is the smallest one, with the characteristic that the activity plummets during the weekend. The area corresponding to this cluster is Porta Romana, which contains the train station with the same name, a station primarily used by commuters into the city. Moreover, the rather isolated areas belonging to one cluster but enclosed by areas in other clusters seem to be explainable and likely not cause by model artifacts. For example, the yellow square in the middle of the green cluster is the location of a large shopping mall. Finally, the spatial dependence parameter ρ has a posterior mean of 0.9 and the posterior mean of the ξ parameter lies close to one, which indicates strong persistence in both space and time.

5.4 Verification of the crowdedness requirements for spatio-temporal model with spatial clustering

5.4.1 P.1 – Overloads are temporary

Figure 8 shows the estimated posterior satisfaction probability and the posterior mean of the robustness measure resulting from the evaluation of property P.1. Note that P.1 defines a property only in terms of a temporal operator where we set $h_{P.1} = 30$ min. That is, we check whether the crowdedness variable stays below a value of $c = 500$ or, in case it exceeds this value, then it must return below it within 30 minutes. When looking at the results it is apparent that the city is roughly split in two macro-areas: the historical and financial center is unlikely to satisfy the property during busy times, while the residential areas are almost always satisfying it. A relevant exception comes from the ⑤ Navigli area (left bottom of the map): it is, in fact, a vibrant area, where many young people live, which has many touristic landmarks and an active commercial area. We can see that this area is consistently violating our requirement over time, although, from a look at the robustness its actual value is close

to zero, meaning that the violation is quite small, making it less concerning from a network capacity perspective.

5.4.2 P.2 – Overloads are local

Figure 9 shows the estimated posterior satisfaction probability and the posterior mean of the robustness measure resulting from the evaluation of property P.2 at three different times of the day. Note that this property is based only on predictions of neighboring locations ($d_{P.2} = 1$ cell) at future time $t + h_{P.2}$, with $h_{P.2} = 10$ min. As one might intuitively expect, the property exhibits high values of satisfaction and robustness for a large area of the city center (there is usually at least an uncrowded area connected to a crowded one). A notable exception is the (3) Duomo area, from which crowds spread towards the other hot-spots at the busiest time of the day (18:20). However, by looking at the posterior predictive mean of the robustness for different time points, we get a more clear understanding about the spatial distribution of the excessive loads. In fact, it is evident that the (3) Duomo is the area that might most likely suffer from excessive crowdedness, without any possibility to enact load-balancing strategies based on the state of nearby locations. Conversely, other areas like the (5) Navigli area, have a much safer spatial behaviour, either because they exceed the threshold only slightly, or because they are surrounded by areas with much lower levels of crowdedness.

5.4.3 P.3 – The network is fault-tolerant

Figure 10 shows the estimated posterior satisfaction probability and the posterior mean of the robustness measure resulting from the evaluation of property P.3 at three different times of the day. Property P.3 enforces the availability of a neighboring uncrowded area (i.e., $d_{P.3} = 1$) consistently for $h_{P.3} = 30$ min. The first thing a reader might notice is the fact that the property exhibits a visual pattern similar to P.1–P.2, except that it is in general less likely to be satisfied. This is to be expected, one can notice when looking at the logic formulae

that **P.3** resembles the structure of the right side of implication (“ \rightarrow ”) in **P.1–P.2**, except that it enforces stricter requirements (there must be an uncrowded area for the next half-hour). This observation shows a key strength of logic for the validation and explainability of specifications: from an informal perspective **P.1** and **P.2** describe different aspects than **P.3**. Yet, the obtained results show that **P.3** could effectively replace **P.1–P.2** as a specification that encompasses both of them. In fact, overall **P.3** summarizes the ideal behavior of a fault-tolerant system. The results of this property clearly show that the city is split into two parts, with the most-touristic part less likely to satisfy the property, while the residential and non-touristic areas are more likely to satisfy it.

5.4.4 **P.4** – Uncrowded reachability

Figure 11 presents the results of verifying property **P.4** for $h_{P.4} = 40\text{min}$ and $d_{P.4} = 4$ cells (approx. 1 km.  circles mark hospitals’ locations, where the property is trivially satisfied in all circumstances. By looking at the picture, an immediate observation is that areas at the corners are simply too far from any of the city center hospitals, meaning that going towards the center from there would be impractical. However, it is interesting to see that, while it is never very easy to get to hospitals in busy times (like at 18:20), the  Central Station is still in a good spot (as it is not too far, and not too crowded), conversely the  Garibaldi Station is in a less favorable location, as it becomes practically inaccessible in crowded times. Even worse is the  Duomo area, which, despite being quite close to a hospital, experiences such high levels of crowdedness that make reaching the hospital almost impossible in crowded times (in the terms of the requirement we have defined), while it is relatively easier in medium-crowded times. Lastly, the always failing areas at the corners of the grid, and at the bottom-center tell us something different: for the spatial configuration we are considering, they always violate the requirement to reach an hospital of the city center in $d_{P.4}$. This can be surprising at first, but a look to the broader map of the city clarifies that they are closer to hospitals that are not in our grid, therefore cannot be fully analyzed

by our model.

6 Discussion and future work

In this paper we propose a framework for predictive model checking and verification, where in addition to usual approaches, we advocate for the specification of concrete (spatio-temporal) properties which the predictions from a model should satisfy. Given trajectories from the Bayesian predictive distribution, the posterior predictive probability of satisfaction and the posterior predictive robustness of these properties can be approximated by verifying the properties on each of the trajectories efficiently using techniques from formal verification methods. Finally, we can evaluate *ex post* the model by comparing the resulting measures with the values in the observed data.

We illustrate the approach by building a Bayesian spatio-temporal model for areal crowdedness extracted from aggregated mobile phone data in the city of Milan and by formulating properties which the crowdedness level in the city network should satisfy in order to robustly withstand critical events. The proposed framework advocates for exploiting the rich information that Bayesian predictive inference offers in the form of draws from the posterior predictive distribution of future values, by evaluating models also based on properties which can be directly translated into decision-making. Therefore, we show-case how different model specifications are then evaluated based on well-known performance measures but also on posterior predictive measures employed in formal verification such as the satisfaction probabilities or the robustness measure.

On a larger scale, by exploiting the synergy between Bayesian modeling and formal verification methods we also advocate for the development and use of explainable algorithms where properties relevant for decision making are incorporated into the data analytic process flow. Therefore, the proposed approach has a clear potential in the area of sustainable cities and urban mobility, as these applications deal with complex systems, with a multitude of

stakeholders and with a pressing need for transparency in the decision-making process. We hope for the illustration in the current paper to open the way to further applications.

Computational details and replication materials

The computations have been performed on 25 IBM dx360M3 nodes within a cluster of workstations. Instruction for downloading the data set as well as an extensive description can be found in [Barlacchi et al. \(2015\)](#). The estimation of the Bayesian models can be performed using R code in the repository <https://github.com/lauravana/CARBayesSTBNP>. The Moonlight tool is available at <https://github.com/moonlightsuite/moonlight>.

Acknowledgments

The authors acknowledge funding from the Austrian Science Fund (FWF) for the project “High-dimensional statistical learning: New methods to advance economic and sustainability policies” (ZK 35), jointly carried out by University of Klagenfurt, Vienna University of Economics and Business (WU), University of Salzburg, TU Wien (in particular the DK LogiCS), and the Austrian Institute of Economic Research (WIFO).

References

Gianni Barlacchi, Marco De Nadai, Roberto Larcher, Antonio Casella, Cristiana Chitic, Giovanni Torrisi, Fabrizio Antonelli, Alessandro Vespiagnani, Alex Pentland, and Bruno Lepri. A multi-source dataset of urban life in the city of Milan and the Province of Trentino. [Scientific data](#), 2(1):1–15, 2015. doi: 10.1038/sdata.2015.55. [19](#), [32](#)

Ezio Bartocci, Luca Bortolussi, Michele Loreti, and Laura Nenzi. Monitoring mobile and spatially distributed cyber-physical systems. In [Proceedings of the 15th ACM-IEEE](#)

International Conference on Formal Methods and Models for System Design, pages 146–155, 2017. doi: 10.1145/3127041.3127050. 8, 10, 12

José M Bernardo and Adrian FM Smith. Bayesian Theory. John Wiley & Sons, 1994. doi: 10.1002/9780470316870. 1

Alba Bernini, Amadou Lamine Toure, and Renato Casagrandi. The time varying network of urban space uses in Milan. Applied Network Science, 4(1):1–16, 2019. doi: 10.1007/s41109-019-0245-x. 4

Pietro Bonato, Paolo Cintia, Francesco Fabbri, Daniele Fadda, Fosca Giannotti, Pier Luigi Lopalco, Sara Mazzilli, Mirco Nanni, Luca Pappalardo, Dino Pedreschi, et al. Mobile phone data analytics against the COVID-19 epidemics in Italy: flow diversity and local job markets during the national lockdown. arXiv preprint arXiv:2004.11278, 2020. 4

Paul-Christian Bürkner, Jonah Gabry, and Aki Vehtari. Approximate leave-future-out cross-validation for Bayesian time series models. Journal of Statistical Computation and Simulation, 90(14):2499–2523, 2020. doi: 10.1080/00949655.2020.1783262. 1

Annalisa Cadonna, Andrea Cremaschi, and Alessandra Guglielmi. Bayesian modeling for large spatio-temporal data: an application to mobile networks, 2019. Working paper. 4, 8

Jonathan Cinnamon, Sarah K Jones, and W Neil Adger. Evidence and future potential of mobile phone data for disease disaster management. Geoforum, 75:253–264, 2016. doi: 10.1016/j.geoforum.2016.07.019. 4

Edmund M. Clarke and E. Allen Emerson. Design and synthesis of synchronization skeletons using branching time temporal logic. In Dexter Kozen, editor, Logics of Programs, pages 52–71, Berlin, Heidelberg, 1982. Springer Berlin Heidelberg. ISBN 978-3-540-39047-3. 3

Valentina Corradi and Norman R. Swanson. Chapter 5 predictive density evaluation. In G. Elliott, C.W.J. Granger, and A. Timmermann, editors, Handbook of Economic

Forecasting, volume 1 of Handbook of Economic Forecasting, pages 197–284. Elsevier, 2006. doi: 10.1016/S1574-0706(05)01005-0. 1

Pierre Deville, Catherine Linard, Samuel Martin, Marius Gilbert, Forrest R Stevens, Andrea E Gaughan, Vincent D Blondel, and Andrew J Tatem. Dynamic population mapping using mobile phone data. Proceedings of the National Academy of Sciences, 111(45):15888–15893, 2014. doi: 10.1073/pnas.1408439111. 4

Georgios E. Fainekos and George J. Pappas. Robustness of temporal logic specifications for continuous-time signals. Theoretical Computer Science, 410(42):4262–4291, 2009. ISSN 0304-3975. doi: 10.1016/j.tcs.2009.06.021. 11

Stefano Favaro and Yee Whye Teh. MCMC for normalized random measure mixture models. Statistical Science, 28(3):335–359, 2013. doi: 10.1214/13-STS422. 8

David T. Frazier, Ruben Loaiza-Maya, Gael M. Martin, and Bonsoo Koo. Loss-based variational Bayes prediction. 2021. 2

Claudio Gariazzo, Armando Pelliccioni, and Maria Paola Bogliolo. Spatiotemporal analysis of urban mobility using aggregate mobile phone derived presence and demographic data: A case study in the city of rome, italy. Data, 4(1), 2019. ISSN 2306–5729. doi: 10.3390/data4010008. 4

John Geweke and Gianni Amisano. Comparing and evaluating Bayesian predictive distributions of asset returns. International Journal of Forecasting, 26(2):216–230, 2010. doi: 10.1016/j.ijforecast.2009.10.007. 2, 9

Md Shahadat Iqbal, Charisma F Choudhury, Pu Wang, and Marta C González. Development of origin–destination matrices using mobile phone call data. Transportation Research Part C: Emerging Technologies, 40:63–74, 2014. doi: 10.1016/j.trc.2014.01.002. 4

Gregor Kastner. Dealing with stochastic volatility in time series using the R package **stochvol**. Journal of Statistical Software, Articles, 69(5):1–30, 2016. doi: 10.18637/jss.v069.i05. 9

Axel Legay, Anna Lukina, Louis Marie Traonouez, Junxing Yang, Scott A. Smolka, and Radu Grosu. Statistical Model Checking, pages 478–504. Springer International Publishing, Cham, 2019. ISBN 978-3-319-91908-9. doi: 10.1007/978-3-319-91908-9_23. URL https://doi.org/10.1007/978-3-319-91908-9_23. 3

Brian G Leroux, Xingye Lei, and Norman Breslow. Estimation of disease rates in small areas: a new mixed model for spatial dependence. In Statistical models in epidemiology, the environment, and clinical trials, pages 179–191. Springer, 2000. doi: 10.1007/978-1-4612-1284-3_4. 7

Laura Nenzi, Luca Bortolussi, Vincenzo Ciancia, Michele Loreti, and Mieke Massink. Qualitative and quantitative monitoring of spatio-temporal properties with sstl. arXiv preprint arXiv:1706.09334, 2017. doi: 10.23638/LMCS-14(4:2)2018. 3

Laura Nenzi, Ezio Bartocci, Luca Bortolussi, Michele Loreti, and Ennio Visconti. Monitoring spatio-temporal properties (invited tutorial). In Jyotirmoy Deshmukh and Dejan Ničković, editors, Runtime Verification, pages 21–46, Cham, 2020. Springer International Publishing. ISBN 978-3-030-60508-7. 12

Jan Peters-Anders, Zaheer Khan, Wolfgang Loibl, Helmut Augustin, and Arno Breinbauer. Dynamic, interactive and visual analysis of population distribution and mobility dynamics in an urban environment using the mobility explorer framework. Information, 8(2):56, 2017. doi: 10.3390/info8020056. 4, 19

J. P. Queille and J. Sifakis. Specification and verification of concurrent systems in cesar. In Mariangiola Dezani-Ciancaglini and Ugo Montanari, editors, International Symposium on Programming, pages 337–351, Berlin, Heidelberg, 1982. Springer Berlin Heidelberg. ISBN 978-3-540-39184-5. 3

Donald B Rubin. Bayesianly justifiable and relevant frequency calculations for the applied statistician. *The Annals of Statistics*, pages 1151–1172, 1984. URL <https://www.jstor.org/stable/2240995>. 1

Aki Vehtari, Andrew Gelman, and Jonah Gabry. Practical Bayesian model evaluation using leave-one-out cross-validation and WAIC. *Statistics and Computing*, 27(2):1413—1432, 2017. doi: 10.1007/s11222-016-9696-4. 1

Zhensheng Wang, Yang Yue, Biao He, Ke Nie, Wei Tu, Qingyun Du, and Qingquan Li. A Bayesian spatio-temporal model to analyzing the stability of patterns of population distribution in an urban space using mobile phone data. *International Journal of Geographical Information Science*, 35(1):116–134, 2021. doi: 10.1080/13658816.2020.1798967. 4

NA Wardrop, WC Jochem, TJ Bird, HR Chamberlain, D Clarke, D Kerr, L Bengtsson, S Juran, V Seaman, and AJ Tatem. Spatially disaggregated population estimates in the absence of national population and housing census data. *Proceedings of the National Academy of Sciences*, 115(14):3529–3537, 2018. doi: 10.1073/pnas.1715305115. 4

Håkan L. S. Younes, Marta Kwiatkowska, Gethin Norman, and David Parker. Numerical vs. statistical probabilistic model checking. *International Journal on Software Tools for Technology Transfer*, 8(3):216–228, June 2006. ISSN 1433-2787. doi: 10.1007/s10009-005-0187-8. 3

Paolo Zuliani, André Platzer, and Edmund M Clarke. Bayesian statistical model checking with application to stateflow/simulink verification. *Formal Methods in System Design*, 43(2):338–367, 2013. doi: 10.1007/s10703-013-0195-3. 4

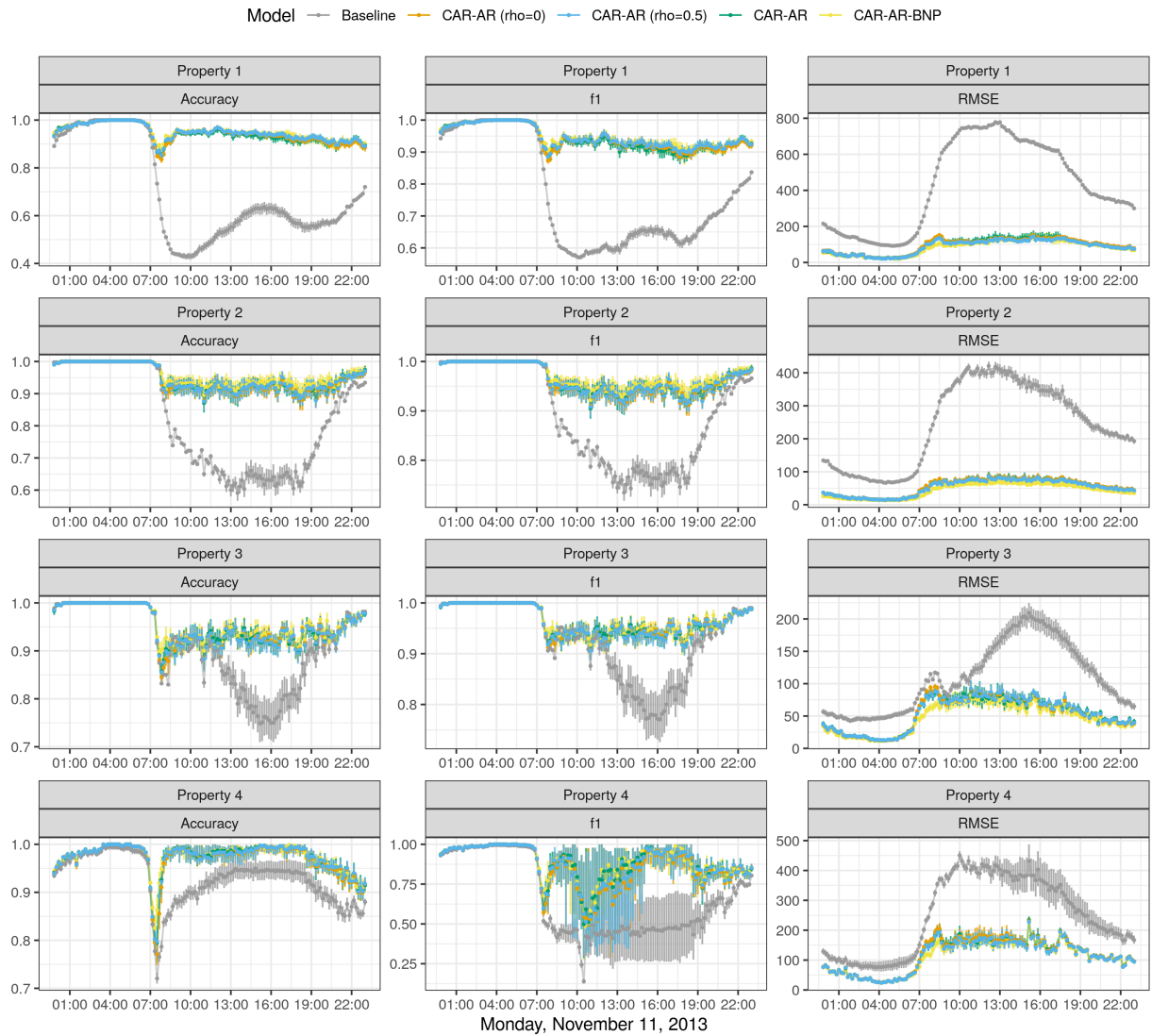


Figure 6: This figure presents the mean accuracy, F1 score for the Bayesian predictive satisfaction measure and the RMSE of the robustness measure (points) with their corresponding 80% credible intervals for a rolling window exercise where the time point of the x -axis represents the end of the training sample.

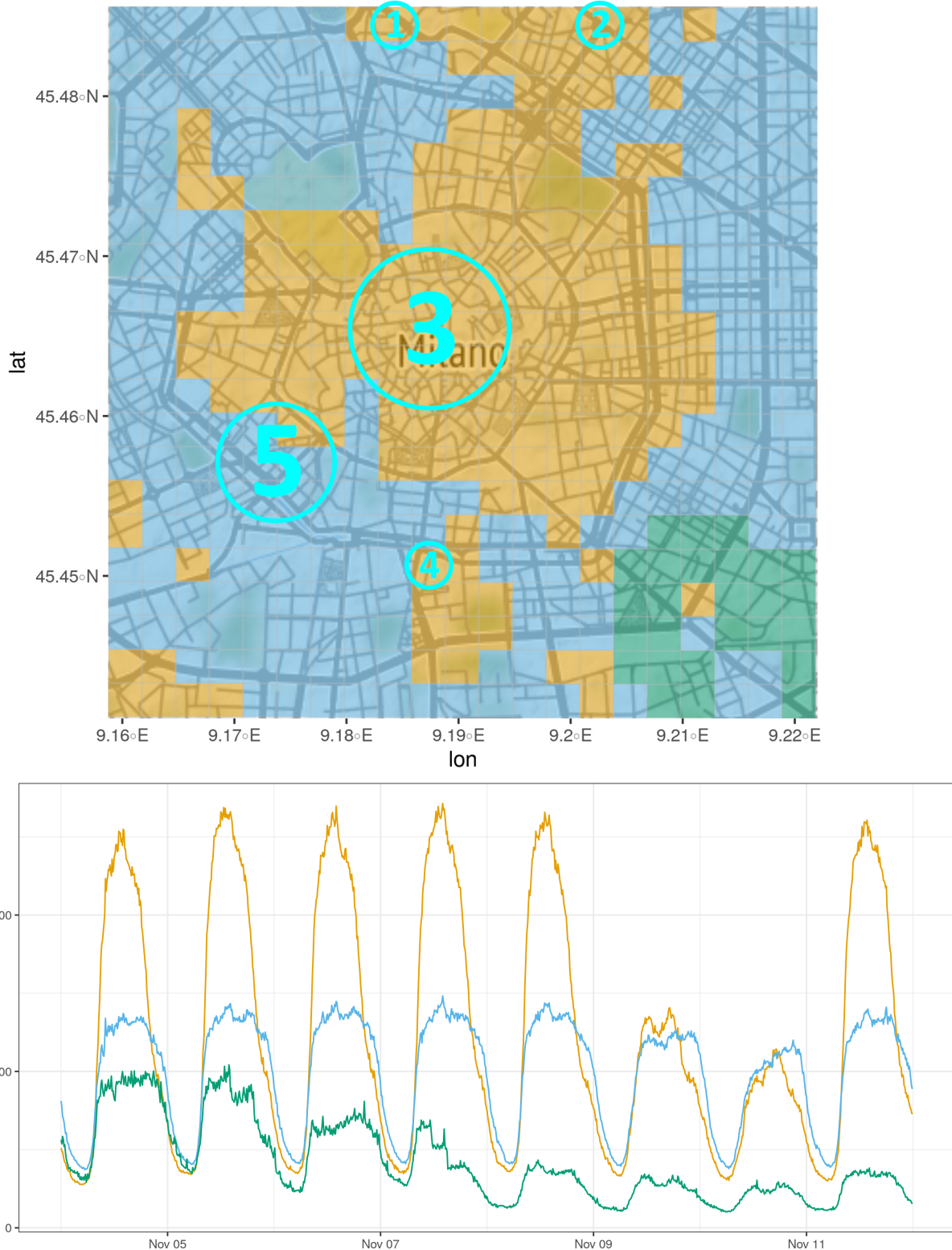


Figure 7: Top panel: Clusters as identified by Binder's loss. Bottom panel: crowdedness measure averaged over all locations in one cluster.

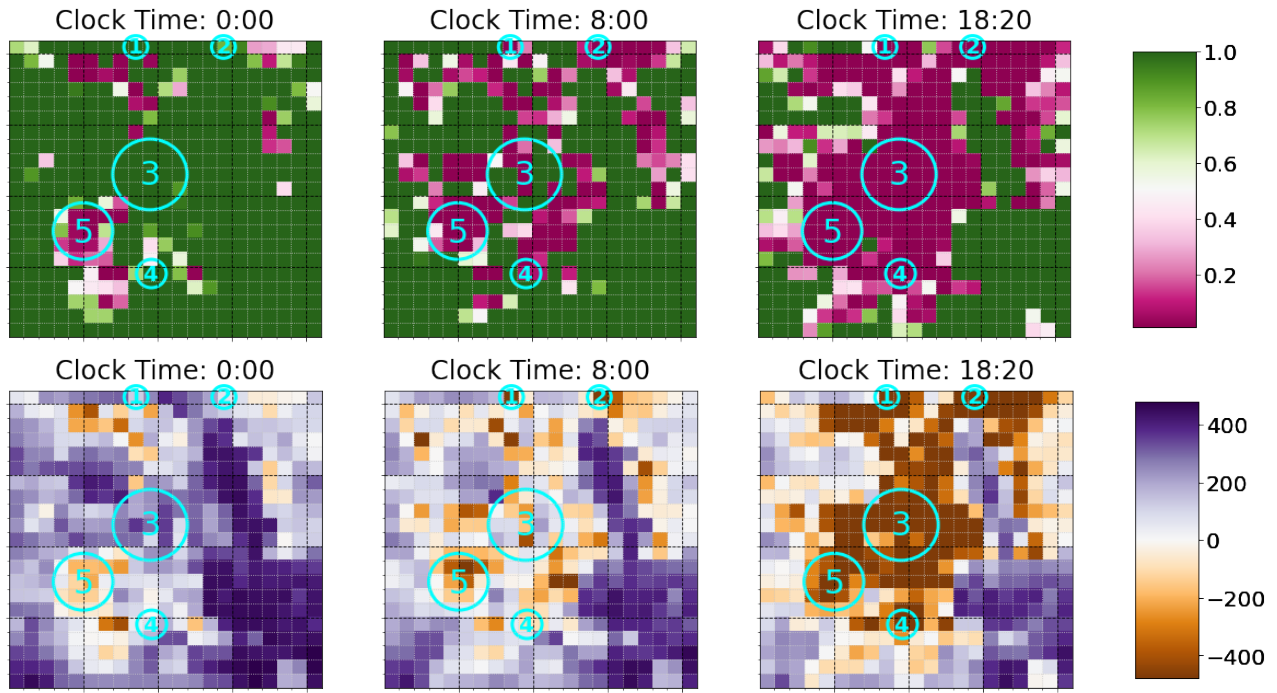


Figure 8: Posterior satisfaction probability (top row) and the posterior mean of the robustness measure (bottom row) resulting from checking for property P.1 at three times of the day.

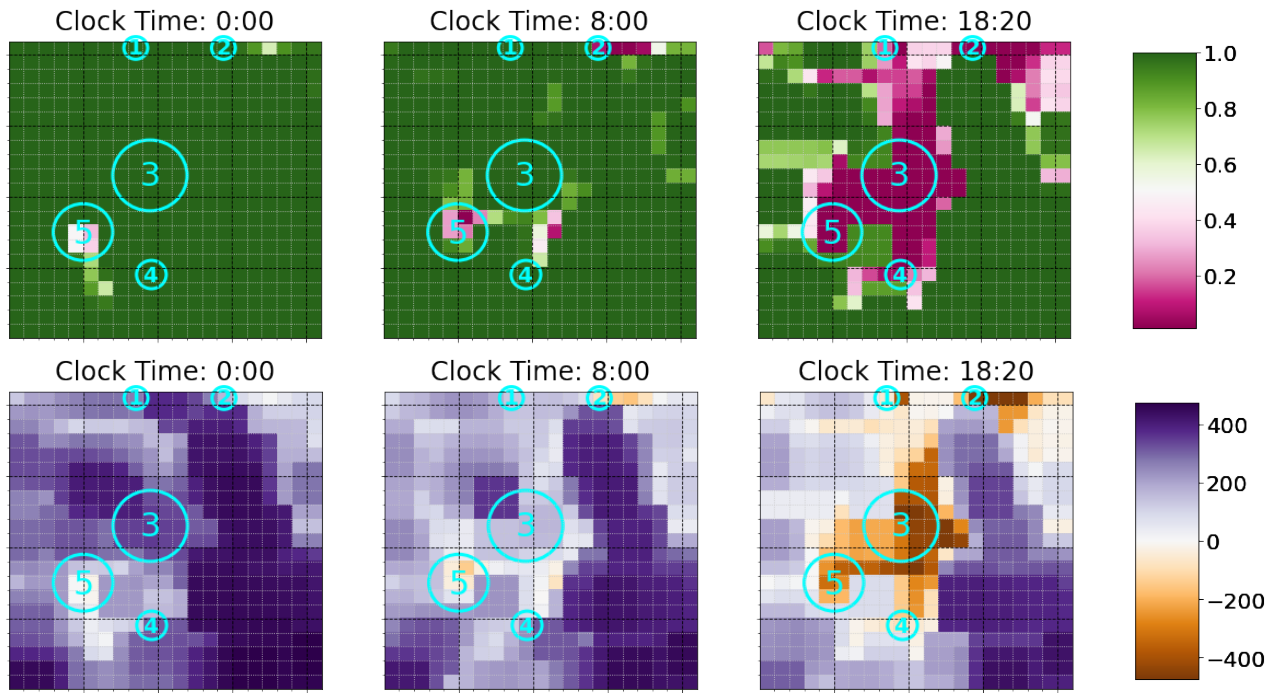


Figure 9: Posterior satisfaction probability (top row) and the posterior mean of the robustness measure (bottom row) resulting from checking property P.2 at three times of the day.

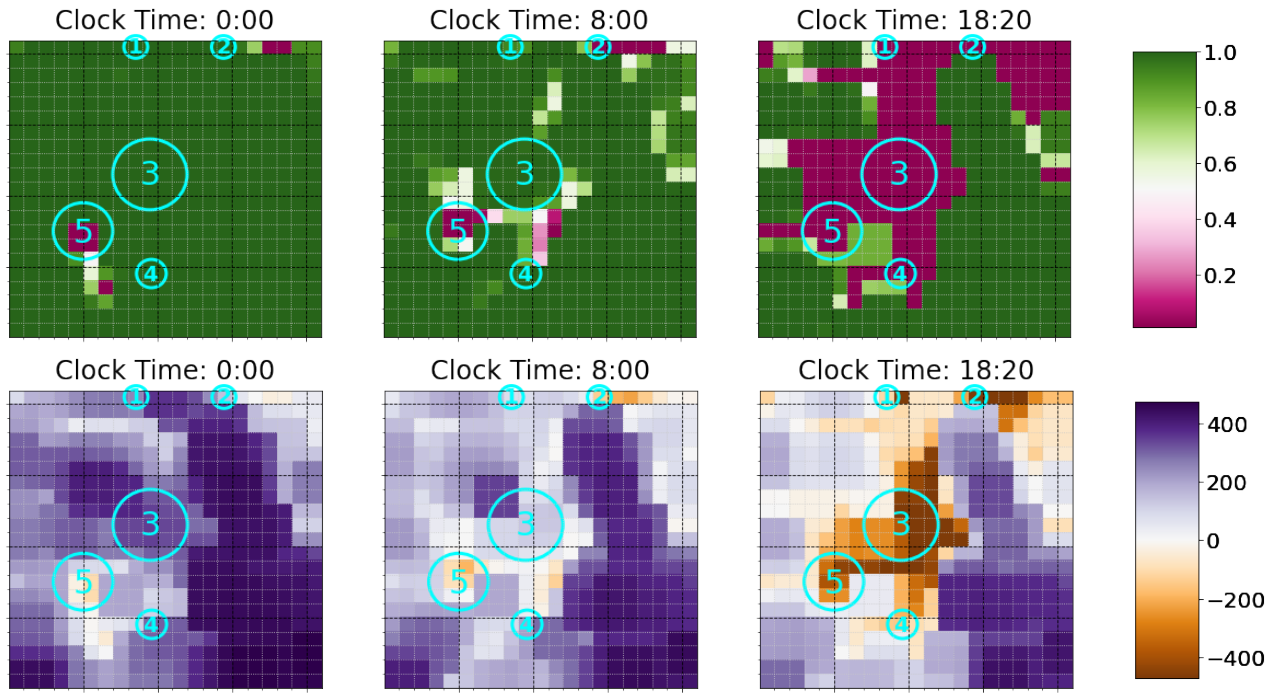


Figure 10: Posterior satisfaction probability (top row) and the posterior mean of the robustness measure (bottom row) resulting from checking property **P.3** at three times of the day.

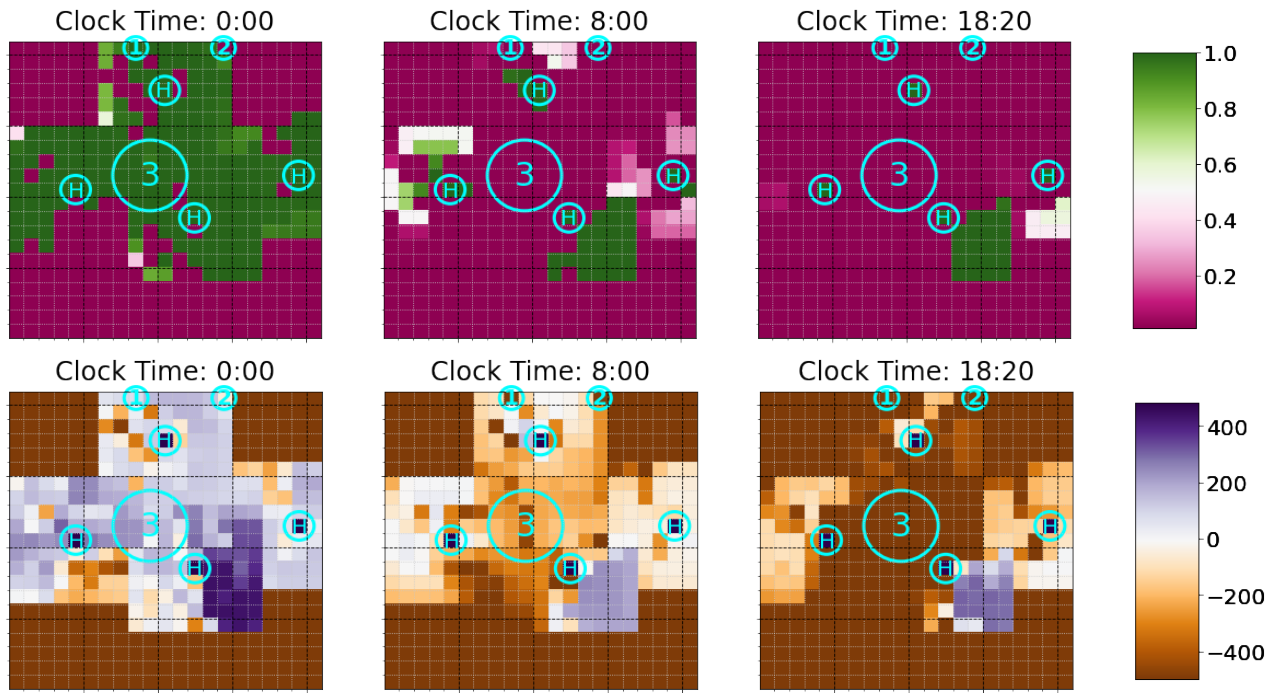


Figure 11: Posterior satisfaction probability (top row) and the posterior mean of the robustness measure (bottom row) resulting from monitoring the property **P.4** at three times of the day.